

Reversible Acceleration of the Corrosion of AISI 304 Stainless Steel Exposed to Seawater Induced by Growth and Secretions of the Marine Bacterium *Vibrio Natriegens**

D. E. NIVENS,* P. D. NICHOLS,* J. M. HENSON,*
G. G. GEESEY,** and D. C. WHITE*

Abstract

Growth of the nonsulfate-reducing marine bacterium *Vibrio natriegens* increased the corrosion current density (CD) of AISI 304 stainless steel (SS) coupons when grown in a marine medium. The corrosion rate, estimated as the corrosion CD (i_{corr}), calculated from the Tafel constants and polarization resistance, increased from 230 to 2900 nA/cm² during a 6-day incubation period with *V. natriegens*. Just before the rapid increase in the corrosion CD, bacterial cells were seen by epifluorescent microscopy after acridine orange staining to colonize the SS surface. On the third day of exposure to seawater, the rapid increase in the corrosion CD correlated with the appearance of extracellular material from the colonizing bacteria, as observed by (1) epifluorescent microscopy, (2) scanning electron microscopy (SEM), and (3) nondestructive analysis of lyophilized biofilms by Fourier transform-infrared spectroscopy (FT-IR) using diffuse reflectance. The extracellular products from the colonizing bacteria correlated with the rapid increase in infrared absorbance at $\sim 1440 \text{ cm}^{-1}$. The IR spectrum of the $\sim 1440 \text{ cm}^{-1}$ component corresponds to authentic calcium hydroxide possibly associated with an organic matrix. Bacterial colonization reached the maximum extent on the fourth day, as monitored by the infrared absorption at $\sim 1660 \text{ cm}^{-1}$, which corresponds to the amide I vibrations in the bacterial proteins as well as in the appearance of the biofilm in epifluorescent microscopy. The increase in the corrosion CD continued after the decrease in the rate of bacterial colonization. Removing the biofilm with sonication and washing decreased the bacterial content of the biofilm monitored at $\sim 1660 \text{ cm}^{-1}$ to a greater extent than the extracellular calcium hydroxide monitored at $\sim 1440 \text{ cm}^{-1}$. This had essentially no effect on the corrosion CD. Sonication followed by extraction with chloroform-methanol removed the extracellular exudation and the bacteria with a 10-fold decrease in the CD. A related bacterium, *V. anguillarum*, showed a smaller increase in corrosion CD that correlated with a smaller increase in infrared absorbance at ~ 1440 and $\sim 1660 \text{ cm}^{-1}$. The present study shows the reversible facilitation of the corrosion of SS exposed to seawater by organisms and extracellular accumulations of nonsulfate-reducing marine bacteria.

Introduction

Corrosion of irons and steels exposed to seawater is a significant problem. The role of microorganisms in facilitating or inhibiting the corrosion of irons or steels has received increasing attention. The materials technology institute of the chemical process industries recently supported a multidisciplinary study group to review the state of the art of microbially influenced corrosion (MIC).¹ The report of this group¹ adds to the limited number of reviews of MIC in the literature.²⁻⁸ This literature deals primarily with the corrosion of irons and steels by

the anaerobic sulfate-reducing bacteria or aluminum by hydrocarbon-degrading organisms. A number of mechanisms have been postulated by which MIC could function with irons and steels.¹ Bacterial films generate organic acids under microaerophilic or anaerobic growth conditions. Organisms capable of oxidizing ferrous or manganous ions to ferric or manganic ions could cause the co-accumulation of highly corrosive ferric and manganic chloride solutions in crevices. This is postulated to lead to severe pitting.⁷ Pseudomonads and other aerobic bacteria have been associated with the accumulation of iron in slimes with MIC. Areas of local oxygen depletion under metabolically active concentrations of bacteria may prevent the normal repair of passive films damaged by halide or mechanical attack. These local accumulations of bacteria can create anaerobic microniches in which the anaerobic sulfate-reducing bacteria can flourish. Other marine aerobic organisms produce extracellular materials that could facilitate cor-

*Submitted for publication February 1985; revised July 1985.

*Dept. of Biological Science and Center for Biomedical and Toxicological Research, Florida State University, Tallahassee, Florida 32306.

**Dept. of Microbiology, Long Beach State University, Long Beach, California 90840.

rosion by generating concentration cells of differing cathodic activities.⁸

A major problem in the study of MIC mechanisms has been that the standard methods of microbiology (i.e., isolation and characterization of bacterial monocultures, which proved useful in the control of infectious disease) have provided little direct evidence for MIC mechanisms. New methods for study of the biomass, community structure, and metabolic activities of microbial consortia involved in ecological processes⁹ can be applied to organisms involved in the MIC of irons and steels exposed to seawater. These methods depend on analyses of *signature* compounds from the membranes of different groups of organisms.⁸ In this study, it will be shown that a complementary method involving Fourier transform-infrared spectrometry (FT-IR) may provide nondestructive analysis of areas on the scale of microorganisms.¹⁰ Using the correlation between microscopy, FT-IR spectroscopy, and corrosion current density (CD) measurements, this study reports the facilitation of corrosion of AISI 304 stainless steel (SS) by the extracellular exudations of the nonsulfate-reducing marine bacterium, *Vibrio natriegens*.

Experimental

Coupons

Disks of AISI 304 SS 1.59 cm (5/8 in.) in diameter, having a face polished with 600 grit powder, were boiled in toluene for 5 min and rinsed with acetone to remove surface films.

Medium

The treated disks were placed in Difco marine broth 2216⁽¹⁾ made to 3.74% (wt/vol), boiled, and filtered through 0.2- μ pore filters before autoclaving. Four disks were placed in 300 mL Erlenmeyer flasks, 100 mL medium was added, and the flasks were capped with SS caps. The flasks were autoclaved at 121 C for 20 min.

Organisms

Cultures of *V. natriegens* and *V. anguillarum* were inoculated using 1 mL from organisms grown for 18 h (stationary phase organisms). Stocks were maintained on agar slants at 5 C. Culture purity was followed microscopically and by Gram stain reactions.

Incubation

Flasks (triple baffled shaker flasks with SS closures) were shaken at 23 C (room temperature) at 80 rpm on a gyratory shaker. At the times indicated, the disks were recovered from the flasks with sterile forceps, rinsed once with filter-sterilized (0.45- μ pore size) artificial seawater at a concentration of 25 ppt, and immediately placed in the filter-sterilized seawater. Within a few minutes, the disks were aseptically transferred from the seawater to the Teflon⁽²⁾ holder of the working electrode with forceps.

Corrosion Current Density

Disks from the control and inoculated flasks were placed in the Teflon holder of the working electrode in the EG&G K105⁽³⁾ flat specimen holder. The corrosion cell contained 600 mL of filter-sterilized seawater that was stirred at 140 rpm at 23 C. The system used twin high density, nonpermeable graphite counter electrodes, and a saturated calomel (reference) electrode (SCE) used with a bridge tube incorporating the ultra-low leakage Vycor⁽⁴⁾ frit. The reference electrode was positioned within 1 mm of the working electrode. The disk was allowed to equilibrate until the drift was ≤ 0.05 mV/s and then scanned at 0.2 mV/s using the EG&G Model 350A⁽⁵⁾ corrosion measurement system. The first disk was cathodically scanned from E_{corr} to -500 mV to obtain the

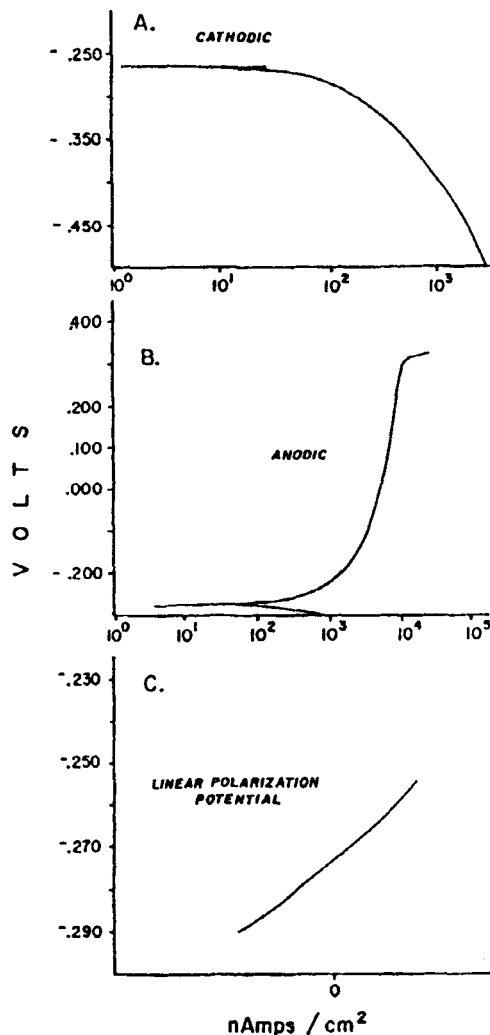


FIGURE 1 — Typical anodic and cathodic linear polarization results, from which Tafel constants were calculated (A and B), and the linear polarization resistance determination results (C) used to determine the corrosion CD.

cathodic Tafel constant (β_c). The second disk was scanned from $E_{\text{corr}} - 10$ to +300 mV to obtain the anodic Tafel constant (β_a). The second disk was then used to measure the polarization resistance (R_p) by scanning from $E_{\text{corr}} - 5$ mV to $E_{\text{corr}} + 5$ mV. I_{corr} was then calculated as $\beta_a \beta_c / 2.3 \times R_p (\beta_a + \beta_c)$.¹¹ Typical plots for anodic and cathodic Tafel constant calculation and linear polarization resistance are shown in Figure 1.

FT-IR Measurement

Disks were stored over P_2O_5 in evacuated desiccators until examined. The disks were then placed in the Spectra Tech diffuse reflectance accessory in the Nicolet 60SX⁽⁶⁾ FT-IR.

Each sample resulted in a single-sided interferogram of 4069 data points that yielded a resolution of 4 cm^{-1} . Signal averaging of 500 scans per sample required 2.5 min of total measurement time. The resulting spectra were ratioed to the appropriate background spectrum. In these experiments, the sample chamber was evacuated for 2 min and purged with dry nitrogen for 2 min before obtaining the spectra.

The spectra were interpreted based on Kubelka-Munk (K-M) analysis¹² and used as an approximation of Beer's law for reflectance spectroscopy.¹³ The liquid-nitrogen cooled, mercury-cadmium-tellurium detector (a range of 5500 to 710

(1)-(5) Registered trade names.

(6) Registered trade name.

cm^{-1}), a mid-range IR global source, and KBr beam splitter were used with the Nicolet 60SX FT-IR. Interferograms were zero filled and apodized by the Haap-Genzel function before the fast Fourier transformation, using Nicolet SX software (TMON version 1.5). Spectra showed identical baselines and are plotted uncorrected.

Scanning Electron Microscopy

Specimens were fixed in glutaraldehyde, relaxed in artificial seawater, critical-point dried¹⁴ or lyophilized, sputter coated, and examined with the JEOL⁽⁷⁾ 100-CX STEM Microscope. Electron diffraction x-ray analysis (EDXA) was performed using the Tracor-Northern⁽⁸⁾ energy dispersive x-ray accessory at the Florida State University STEM facility.

Epifluorescence Microscopy

The biofilm on lyophilized disks was stained with 0.2% (wt/vol) filtered acridine orange¹⁵ and photographed using the Zeiss⁽⁹⁾ Model GFA epifluorescence microscope with an attached Olympus⁽¹⁰⁾ OM-1 camera back and filter set numbers 48-77-07 and 99-03 (Zeiss) to provide the proper wavelengths.

Results

Corrosion With Colonization

Colonization by the nonsulfate-reducing bacterium *V. natriegens* of polished surfaces of AISI 304 SS disks in a seawater medium over a 6-day period resulted in a 13-fold increase (from 230 to 2900 nA/cm^2) in the corrosion CD when compared to the control coupons (Figure 2). The sequence of colonization can be followed in micrographs after staining with acridine orange and exposure to epifluorescent illumination (Figure 3). Bacteria initially attach to the surface as individual cells

(7)-(10)Registered trade names.

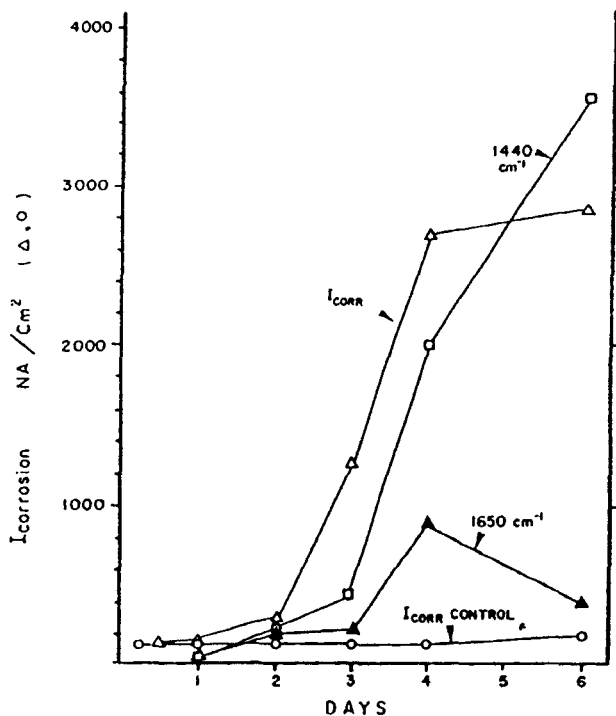


FIGURE 2 — Relationship between the corrosion CD and absorbance at ~ 1440 and $\sim 1660 \text{ cm}^{-1}$ of the biofilm on AISI 304 SS exposed to a seawater medium in the presence of *V. natriegens*.

[Figure 3(A)]. Microcolonies can be detected by 24 h [Figure 3(B)]. At 72 h, the microcolonies are obscured by an extracellular exudation [Figure 3(D)]. This extracellular exudate increasingly covers the bacterial colonies as the exposure is continued. The initiation of the rapid increase in the corrosion CD corresponds to the production of the extracellular material at 72 h [Figures 2 and 3(D)]. Nondestructive analysis of the biofilms on the disks by FT-IR spectroscopy shows two significant changes with time (Figure 4). The absorption at $\sim 1660 \text{ cm}^{-1}$ detects the presence of proteins in the bacteria. Other studies from this laboratory have shown that the intensity of this absorption correlates with the numbers of bacteria in biofilms.¹⁰ The biofilms generated by *V. natriegens* also show a prominent broad absorption centered at $\sim 1440 \text{ cm}^{-1}$. The increase in $\sim 1440 \text{ cm}^{-1}$ parallels the increase in corrosion CD (Figure 2) and the appearance of extracellular exudation (Figure 3). The increase in bacterial numbers, as monitored by the absorbance at $\sim 1660 \text{ cm}^{-1}$, follows the increase in the corrosion CD for the initial portion of the experiment (Figure 2).

Formation of Exudate on Surfaces

V. natriegens grown to the stationary phase on AISI 304 SS coupons, commercial aluminum foil, or the surface of Teflon sheets shows a similar spectrum featuring the same prominent absorption at $\sim 1440 \text{ cm}^{-1}$ seen in Figure 4 (lower spectrum).

Effects of Biofilm Removal on the Corrosion Current Density

A biofilm was generated on AISI 304 SS disks and then removed by a combination of washing, sonication, and solvent extraction (Figure 5). The bacterial cells were differentially removed with washing and sonication, as evidenced by a 40-fold decrease in the $\sim 1660 \text{ cm}^{-1}$ absorption compared to a 15-fold decrease in the extracellular exudate monitored at $\sim 1440 \text{ cm}^{-1}$. Chloroform-methanol extraction with additional sonication induced a further 43-fold decrease in extracellular exudate ($\sim 1440 \text{ cm}^{-1}$), a total removal of absorbance resulting from cellular protein at $\sim 1660 \text{ cm}^{-1}$, and a 10-fold decrease in the corrosion CD.

Corrosion by *V. anguillarum*

The related marine *Vibrio*, *V. anguillarum*, also induced corrosion of AISI 304 SS disks (Figure 6). The increase in the corrosion CD was less than that produced by *V. natriegens* over the same time interval. The decreased corrosion induced by *V. anguillarum* correlated with decreased extracellular exudate ($\sim 1440 \text{ cm}^{-1}$) and bacterial biomass ($\sim 1660 \text{ cm}^{-1}$). The FT-IR spectra after 96 h of exposure showed features essentially similar to those illustrated in Figure 4.

The corrosion CD after 24 h of exposure, when compared to the logarithm of the infrared absorption expressed in K-M units, showed linear correlation coefficients for *V. natriegens* of $r = 0.87$ with the $\sim 1440 \text{ cm}^{-1}$ band and $r = 0.85$ with the amide I band at 1660 cm^{-1} (Figure 5). The linear correlation coefficients for *V. anguillarum* were $r = 0.94$ for the $\sim 1660 \text{ cm}^{-1}$ band and $r = 0.99$ for the $\sim 1440 \text{ cm}^{-1}$ band (Figure 6).

Nature of the Extracellular Exudate

Scanning electron microscopy of the biofilm formed by *V. natriegens* and its extracellular exudate of the SS surface clearly shows the *Vibrios* (rod-shaped bacteria) and the extracellular material at a magnification of 2000 (Figure 7). At increasingly higher magnifications, the structure of the extracellular material showed rosette-shaped crystals. The square indicated in the extracellular material in Figure 7(C) indicates the area subjected to x-ray analysis. The x-ray analysis showed that no heavy metals were present. Only calcium and chloride gave significant signals. The infrared spectrum indicates a close similarity between the extracellular accumulations with absorption centered at 1440 cm^{-1} and between authentic calcium hydroxide (Figure 8).

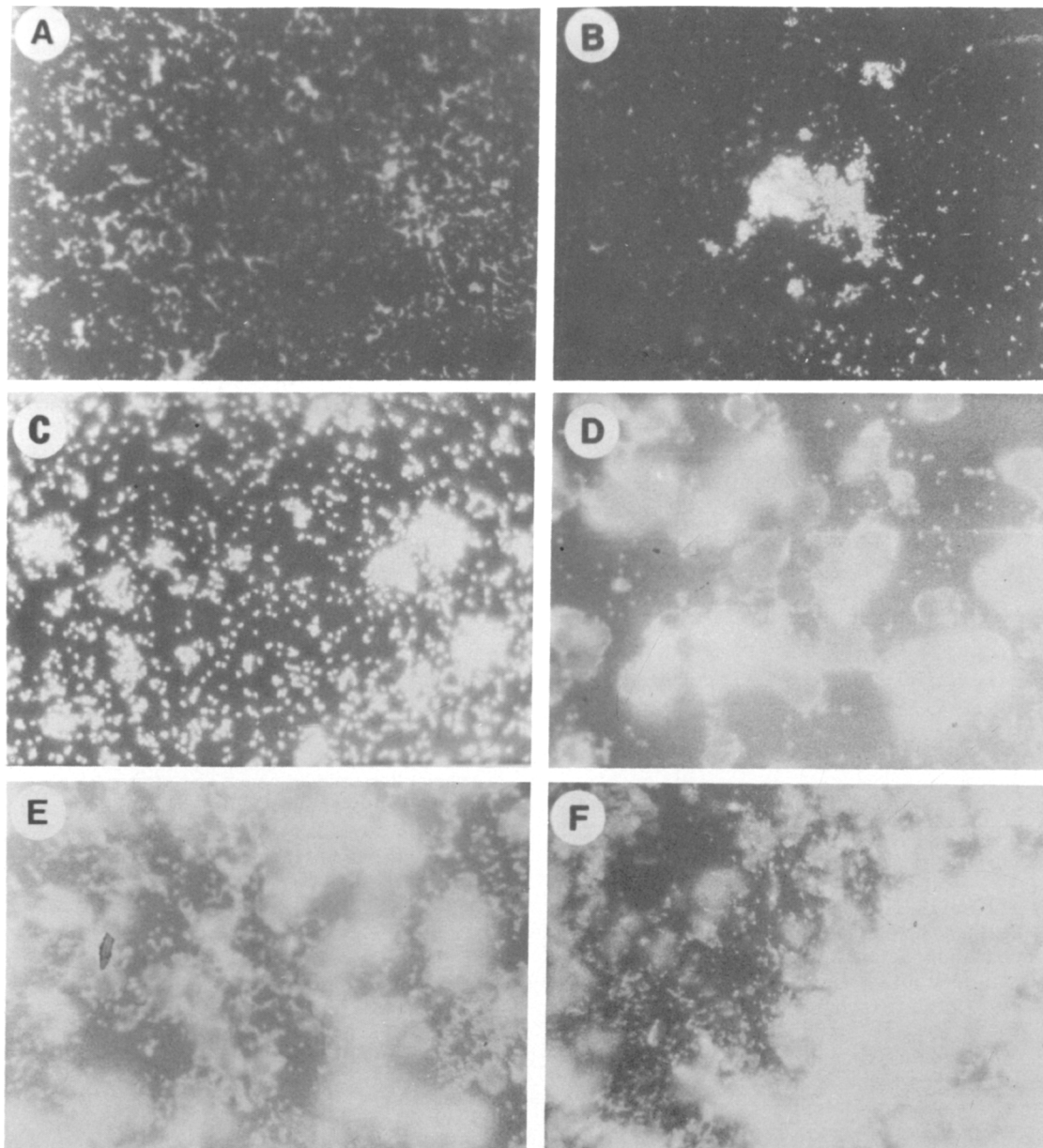


FIGURE 3 — Micrographs of *V. natriegens* colonizing AISI 304 SS surfaces stained with acridine orange and exposed to epifluorescent illumination at 400X for (A) 12 h, (B) 24 h, (C) 48 h, (D) 72 h, (E) 96 h, and (F) 144 h, showing the rapid accumulation of extracellular material.

Discussion

Mechanisms of Microbially Influenced Corrosion

There are several mechanisms by which microbes have been shown to facilitate the corrosion of steels. Some bacteria generate mineral acids such as H_2SO_4 or HNO_3 by oxidizing reduced sulfur or nitrogen compounds in the presence of air. The *Thiobacilli* readily attack surfaces when grown in the presence of reduced sulfur and oxygen.¹⁶ In areas in which microbes can accumulate, the respiratory activities of heterotrophic bacteria create anaerobic microniches in which anaerobes can flourish. In fine muddy sediments, the proportions of fermentative anaerobes containing the plasmalogen phospholipids are at least 10-fold greater in the aerated top portions of the sediments than in the deeper anaerobic layers.^{17,18} In these anaerobic environments, fermentative bacteria create organic acids and carbonic acid, which can be sufficiently corrosive to weather rocks into soils. The increase in corrosion of nickel by obligately thermophilic bacteria may

be the result of isobutyric and isovaleric acid elaboration.¹⁹ Some anaerobes generate hydrogen that may contribute to the embrittlement of steels.²⁰ In the presence of sulfate, such as in seawater, the sulfate-reducing bacteria generate hydrogen sulfide in these anaerobic niches with notorious consequences for corroding metals.

The present study examined a different mechanism for corrosion involving the production of extracellular materials by aerobic marine bacteria. Some of these organisms such as *Gallionella*, *Spherotilus*, and some *Pseudomonads* can selectively oxidize or reduce iron and strongly bind it to extracellular polymers. Both of the *Vibrios* used in this study clearly induce the increased corrosion CD that correlates with colonization of the SS surface (Figures 2 and 7). However, with the MIC developed with the bacteria in such thin films, it is unlikely that anaerobic conditions would be created (Figures 3 and 7). Both of these organisms secreted extracellular material, the appearance of which correlated with a great increase in the absorbance at $\sim 1440\text{ cm}^{-1}$. The formation of exudate correlated with the increase in corrosion CD, but the exudate showed no evidence of binding iron. Clearly, MIC

VIBRIO NATRIEGENS CORROSION EXPT.

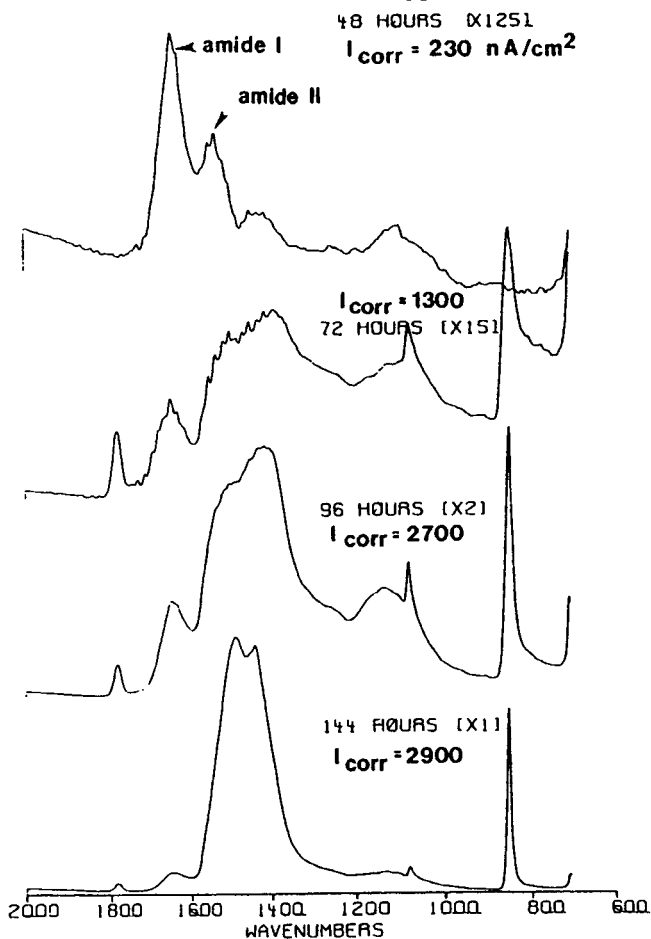


FIGURE 4 — FT-IR of biofilms induced by the colonization of *V. natriegens* on AISI 304 SS surfaces. [Values] indicate multiplication factors for the abscissa compared to the bottom spectrum.

must involve a different mechanism.

The rapid increase in bacteria and extracellular material is related to the increase in the corrosion CD (Figures 2 and 6). Late in the growth cycle, the extracellular material may make the greatest contribution to MIC, as suggested from the effect of its removal on the corrosion CD (Figure 5). The related organism, *V. anguillarum*, forms a similar extracellular material, with absorption at $\sim 1440\text{ cm}^{-1}$. This evidence indicates a role for the extracellular excretions in facilitating corrosion. X-ray analysis of this material showed no concentration of iron or chromium, so the exudate must facilitate corrosion by a mechanism other than strongly chelating the metal ions released from the SS surface. This material is also secreted by *V. natriegens* when it colonizes aluminum or Teflon surfaces where iron binding would be unlikely.

The present authors propose that the uneven distribution of biomass evident in the photomicrographs (Figures 3 and 7) creates concentration cells that differ in cathodic activity. This difference in cathodic activities creates metal surfaces relatively more anodic and could then facilitate corrosion. It is also possible that the increase in extracellular material creates microanaerobic sites, and that the organisms locally generate organic acids and carbonic acid. However, it is believed that this is unlikely, at least in the initial process of colonization.

The extracellular material with the IR maximum centered at $\sim 1440\text{ cm}^{-1}$ has the spectrum of authentic calcium hydroxide. The calcium hydroxide associated with the growth of the *Vibrios* shows differences in the major absorbances possibly associated with an organic matrix (Figure 8). Authentic calcium hydroxide deposited on the SS coupons did not increase the corrosion CD. It appears that the combination of

VIBRIO NATRIEGENS CORROSION EXPERIMENT:

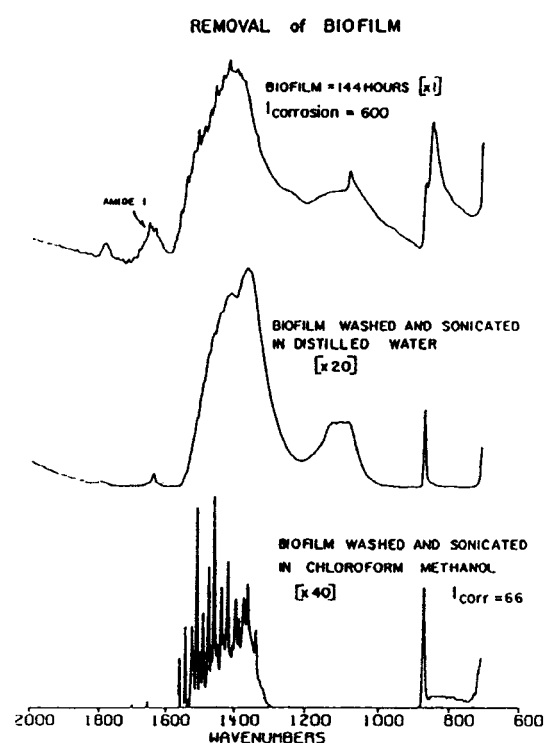


FIGURE 5 — FT-IR spectra and corrosion CD changes of biofilms formed by *V. natriegens* after washing and sonication (middle panel) and after a further sonication and chloroform-methanol extraction (lower panel). [Values] indicate multiplication factors for the abscissa compared to the topmost spectrum.

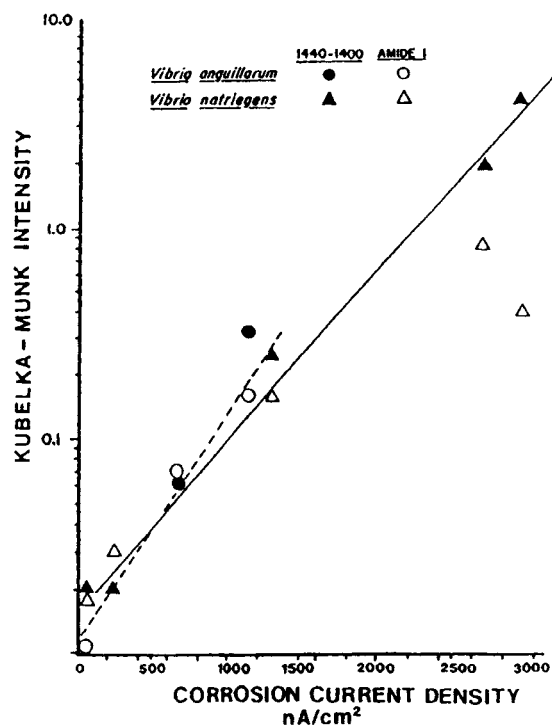


FIGURE 6 — Relationship between the corrosion CD and the log of the infrared absorption of bacteria (amide I = $\sim 1660\text{ cm}^{-1}$) (open symbols and dotted line) and extracellular material ($\sim 1440\text{ cm}^{-1}$) (closed symbols and solid line) of *V. natriegens* (triangles) and *V. anguillarum* (circles) grown on AISI 304 SS coupons in marine broth 2216 (3.74% w/vol).

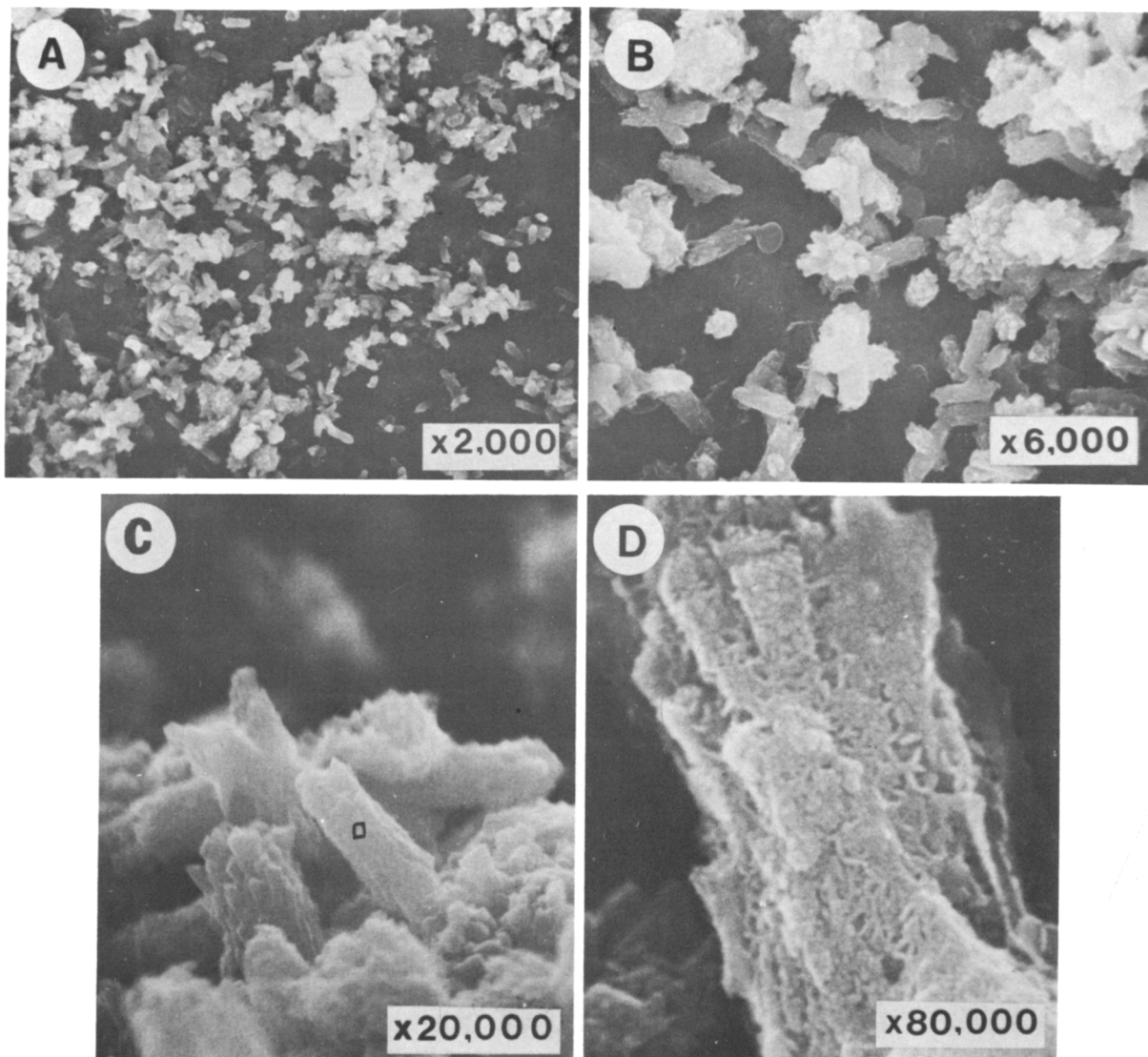


FIGURE 7 — Scanning electron micrographs of the biofilm generated by *V. natriegens* grown on AISI 304 SS disks for 144 h [see (Figure 3(F)), showing progressively greater magnifications of the rosette-shaped crystals. The square in panel C indicates the area analyzed for elemental composition by EDXA that showed calcium and chloride as significant ions.

the modified calcium hydroxide accumulated by the bacteria together with the bacteria are necessary to significantly increase the corrosion CD.

Preliminary work from this laboratory has shown that facilitation of corrosion of AISI 304 SS by the bacterium *Pseudomonas atlantica* may also use the generation of cells of different cathodic activity in facilitating corrosion. This organism is an obligate aerobe that generates uronic acid containing extracellular polysaccharide²¹ with an IR absorption at $\sim 1150\text{ cm}^{-1}$.¹⁰

This study demonstrates the power of the FT-IR in defining the chemical composition of biofilms that is fast, sensitive, nondestructive, and capable of examining areas $25\text{ }\mu\text{m}$ in diameter.¹⁰ This research illustrates its usefulness in examining mechanisms for MIC. If a method of measuring corrosion CD could be miniaturized to the same extent, the generation of concentration cells by accumulation of extracellular materials could be directly demonstrated. The use of galvanically coupled electrodes (one inoculated and the other sterile) in two vessels connected by a membrane with $0.1\text{-}\mu\text{m}$ pores may provide a means to test smaller surfaces with great sensitivity.¹⁹

Acknowledgments

The FT-IR was purchased with funds from grant N00014-83-G0166 from the Department of Defense, University Instrumentation program through the Office of Naval Research. The EG&G corrosion measurement system was purchased with funds from program 0617 of the Florida State University Foundation. The research was supported by contract N00014-83-K0056 from the Department of the Navy, Office of Naval Research. The authors thank T. J. Fellers for the scanning electron microscopy and M. Trexier for preparation of the figures. They also thank R. R. Colwell, University of Maryland, for the gift of the cultures of *Vibrio natriegens* and *V. anguillarum*.

References

1. D. H. Pope, D. J. Duquette, A. H. Johannes, P. C. Wayner, *Materials Performance*, Vol. 24, No. 4, p. 14, 1984.
2. J. Chantereau, *Corrosion Bacterienne*, 2nd ed., Paris: Techniques et Documentation, Paris, France, 1980.
3. V. Kucera, *Microbiological Corrosion—A Literature Survey*, Swedish Corrosion Institute, Stockholm, Sweden, 1980.
4. J. D. A. Miller, A. K. Tiller, *Microbial Aspects of Metallurgy*, Elsevier, New York, New York, 1970.

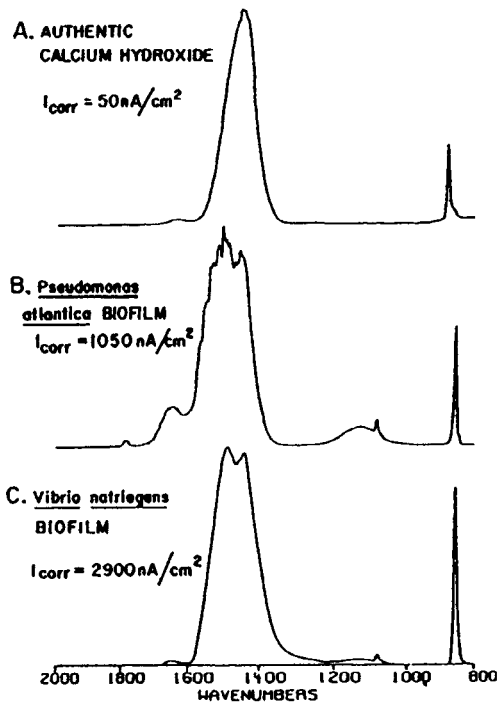


FIGURE 8 — FT-IR spectra of authentic calcium hydroxide (top) and the extracellular accumulation associated with *V. natriegens* (bottom).

5. W. P. Iverson, Microbial Iron Metabolism, Academic Press, New York, New York, 1974.
 6. G. H. Booth, F. Wormwell, 1st Int. Cong. Met. Corros., London, Butterworths, London, England, 1962.

7. G. Kobrin, Materials Performance, Vol. 16, No. 7, p. 38, 1976.
 8. D. C. White, CORROSION/82, Paper No. 55, National Association of Corrosion Engineers, Houston, Texas, 1982.
 9. D. C. White, "Microbes in their Natural Environment," Soc. Gen. Microbiol. Symp., Vol. 34, p. 37, 1983.
 10. P. D. Nichols, J. M. Henson, J. B. Guckert, D. E. Nivens, D. C. White, J. Microbiol. Methods, Vol. 4, p. 79, 1985.
 11. M. Stern, A. L. Geary, J. Electrochem. Soc., Vol. 104, p. 56, 1957.
 12. P. Kulbelka, F. Munk, Zeit. Tech. Phys., Vol. 12, p. 593, 1931.
 13. H. G. Hecht, Appl. Spectroscopy, Vol. 34, p. 161, 1980.
 14. S. J. Morrison, J. D. King, R. J. Bobbie, R. F. Becthold, D. C. White, Marine Biology, Vol. 41, p. 229, 1972.
 15. R. Zimmerman, L. Meyer-Reil, Kieler Meersforsch, Vol. 30, p. 24, 1974.
 16. W. Sand, E. Bock, D. C. White, CORROSION/84, Paper No. 96, National Association of Corrosion Engineers, Houston, Texas, 1984.
 17. D. C. White, W. M. Davis, J. S. Nickels, J. D. King, R. J. Bobbie, Oecologia (Berlin), Vol. 40, p. 51, 1979.
 18. D. C. White, R. J. Bobbie, J. D. King, J. S. Nickels, P. Amoe, Methodology for Biomass Determination and Microbial Activities in Sediments, ASTM STP 673, ASTM, Philadelphia, Pennsylvania, p. 87, 1979.
 19. B. Little, M. Walch, P. Wagner, S. M. Gerchakov, R. Mitchell, 6th Int. Cong. Marine Corros. and Fouling, Athens, Greece, p. 511, 1984.
 20. M. Walch, R. Mitchell, CORROSION/83, Paper No. 249, National Association of Corrosion Engineers, Houston, Texas, 1983.
 21. D. J. Uhlinger, D. C. White, Appl. Environ. Microbiol., Vol. 45, p. 64, 1983.

PROCEEDINGS: THE FOURTH INTERNATIONAL CONGRESS ON METALLIC CORROSION AND THE FIFTH INTERNATIONAL CONGRESS ON METALLIC CORROSION

SPECIAL OFFER

These books are a must for any corrosion library with over 320 technical papers between them, presented by experts in the field. Now the two book set is available at a sixty percent discount over their original price. It's an opportunity not to be missed.

Proceedings: Fourth International Congress on Metallic Corrosion

This book contains 116 technical papers presented during the fourth International Congress on Metallic Corrosion held on September 7-14, 1969 in Amsterdam. The major topics include: Mechanical Influences on Corrosion * Atmospheric Corrosion * Microstructure and Corrosion * Corrosion in Special Environments * Passivation and Anodic Protection * Cathodic Protection * Non-Metallic Coatings * Metallic Coatings * and Miscellaneous.

Proceedings: Fifth International Congress on Metallic Corrosion

The fifth International Congress on Metallic Corrosion was held May 21-27, 1972, in Tokyo, Japan. It was supported by the Science Council of Japan, the Ministry of Education, and the Japan Corrosion Council among others. Emphasis was placed on the creation of meaningful dialogue to help bridge the gap between corrosion science and corrosion engineering. The scientific program of the fifth Congress consisted of 15 section meetings: Electrochemical Processes including Anodic Dissolution * Passivity * Corrosion Cracking and Fracture * Inhibitors * Cathodic and Anodic Protection * Protective Coatings * High Temperature Oxidation * Atmospheric Corrosion * Sea Water Corrosion * Underground Corrosion * Corrosion in Power Industries * Corrosion in Process Industries * Corrosion in Special Environments * Corrosion Testings * Corrosion Education with Panel Discussions. At these section meetings, 207 papers were delivered by corrosion scientists and engineers from 27 different countries. Nearly all of the papers are included here along with 5 plenary lectures, representing an extremely valuable compilation of expert information from around the world.

Item #51046 and Item #51081 \$52.00 for the set, NACE members and nonmembers.

Fourth Congress: 8 1/2 x 11" * hard cover * 822 pages plus index * figures, tables, references. [Item #51046]

Fifth Congress: 8 1/2 x 11" * hard cover * 1137 pages plus author index * figures, tables, references. [Item #51081]

Available from: NACE Order Department, P.O. Box 218340, Houston, Texas 77218

Credit cards accepted on phone orders: American Express, VISA, MASTERCARD®. Credit card orders subject to approval. Call NACE: 713/492-0535

Note: All orders from Texas must include 5.125% sales tax. All orders within the USA must include \$3.00 for handling; orders from outside the USA must include \$5.00 for handling. All orders from Mexico and overseas must be prepaid. Proforma invoices will be sent for any orders which are not prepaid. Remittances from foreign countries must be by international money order or bank draft in USA funds.